RESEARCH

Upgrading the Compressor Stage of the CAT250TJ Micro Gas Turbine Engine

Hano van Eck[1] · Sybrand Johannes van der Spuy[1]

Abstract

Due to their simplicity and relative ease of manufacture, single-stage centrifugal and mixed flow micro gas turbine (MGT) engines are preferred in thrust-based remotely piloted aerial vehicles. A single-stage mixed-flow compressor upgrade for the 200 N CAT250TJ MGT engine is numerically evaluated and presented. An in-house developed mean line application and commercial CFD software is used for the design and performance evaluation of the proposed upgrade configurations. The CAT250TJ – Gen1 engine features a single-stage centrifugal compressor, annular combustor, and single stage axial turbine. Apart from an upgraded impeller, a new crossover diffuser configuration is introduced to replace the wedge-type, straight outlet diffuser configuration of the Gen1 engine. The new single vane crossover diffuser configuration provides a design point total-to-total efficiency and pressure ratio increase of 8.3% and 12.1%, respectively. A disadvantage of a single-vaned crossover diffuser compared to legacy diffusers is a narrower operating range. To alleviate this issue, various combinations of tandem and splitter vane crossover diffuser configurations are proposed. These provide an enhanced operating range, comparable with the operating range displayed by the Gen1 configuration. A turbine power matching analysis is additionally completed to ensure proper compressor integration. Gas turbine cycle software is used to evaluate the on-engine performance of the upgraded compressor configurations. It is shown that the new baseline, single vane crossover diffuser configuration provides a 10.74% increase in design point static thrust.

Keywords Micro gas turbine · Mixed-flow compressor · Crossover diffuser · Tandem vane · 1D App

1 Introduction

Micro gas turbine (MGT) engines are popular for use in smaller thrust-based aerial platforms. These include radio-controlled aircraft, unmanned aerial vehicle (UAV) systems, long-range stand-off weapon (SOW) systems and target drones. In these applications, an optimal balance between platform size and weight is required, leading to the need for a high-power-density propulsion system. The high thrust-to-weight ratios attributed to MGT engines make them well-suited for such applications [1]. Centrifugal compressors are traditionally employed in smaller MGT applications due to their low cost, reliability, fewer parts, and higher per stage

pressure ratios and efficiencies when compared to axial flow compressor stages [2]. Centrifugal compressors do, however, pass lower mass flow rates compared to similar axial flow machines [3]. Additionally, due to their design, centrifugal compressors have larger frontal areas compared to axial flow machines. This invariably leads to higher total drag values when fitted to aerial platforms [4]. Compressor design plays an important role in overall engine performance. For this reason, artificial intelligence methods are already widely used by modern compressor design teams [5].

Mixed flow compressors feature an impeller with a meridional exit angle of lower than 90°. They fall between pure centrifugal and axial flow configurations and therefore combine the advantages of both these extreme configurations. Mixed flow compressor stages can pass higher mass flow rates compared to a similar centrifugal configuration while still producing high-pressure ratios needed for single-stage designs [6]. An added advantage of a mixed-flow compressor configuration is a smaller frontal area, which leads to lower overall drag values. They further display wider

✉ Hano van Eck
hvaneck@sun.ac.za

Sybrand Johannes van der Spuy
sjvdspuy@sun.ac.za

1 Department of Mechanical and Mechatronic Engineering, Stellenbosch University, Stellenbosch, South Africa

operating ranges than comparable centrifugal compressor configurations [7].

The reduced impeller exit meridional angle (α_{C2}—see Fig. 1) attributed to a mixed flow configuration leads to a reduction in the Coriolis force imparted on the flow and exit flow slip, assuming the rotational velocity and impeller exit radius remain unchanged [8]. The tangential component of the relative impeller exit velocity is therefore reduced. Assuming a constant rotational velocity and meridional exit velocity, the effect is a higher absolute impeller exit velocity. This, in conjunction with the increased axial velocity component inherent to the mixed flow design, increases the mass flow capacity of the impeller, leading to higher achieved thrust levels [6].

Due to size limitations, the design and performance of the diffuser largely dictates the performance of a MGT compressor stage, both in terms of design point performance (efficiency and pressure ratio) and operating range. Compared to vaneless diffusers, vaned diffusers provide higher efficiencies [9]. Therefore, vaned diffuser configurations are preferred in MGT engines. Early mixed-flow compressor research showed possible diffuser-matching issues [10]. To alleviate this, vaneless diffusers were initially used. The

use of mixed-flow compressors would therefore seem counterintuitive in MGT engines. Crossover diffuser configurations provide a solution in this regard. The continuous vane design provides a gradual flow turning (radial and tangential to axial) and diffusion solution. Crossover diffuser configurations provide better diffusion performance than similar conventional diffuser configurations (Fig. 2a) [11]. Conventional diffusers typically display flow breakaway and efficiency losses in the vaneless bend section. A crossover diffuser configuration (Fig. 2b) is therefore well suited for use in a MGT mixed flow compressor stage.

A disadvantage of the long flow passages attributed to crossover diffusers is their reduced operating range due to boundary layer growth. A pressure gradient forms on the suction side of the diffuser vane close to the leading edge, which induces a secondary flow from the hub to the shroud. This leads to flow separation towards the rear of the diffuser passage [13]. The effect is aggravated by an increase in passage length. The boundary layer growth in the flow passage can be controlled by introducing a tandem vane configuration [14]. The slot created by the tandem vanes (see Fig. 3) allows the boundary layer to be re-energised, better controlling the boundary layer at various operating points and therefore the overall operating range. Van Eck [15] numerically investigated various tandem vane crossover diffuser configurations and their effect on compressor design point performance and operating range. It was shown that a low solidity front vane configuration displayed a marked increase in choke margin. It was further found that a 75% second row relative tangential shift provided the best overall results, regardless of relative front vane length. A 70–75 configuration provided superior exit tangential velocity results. The designation 70–75 refers to a tandem vane diffuser having a front vane length 70% relative to the total diffuser vaned
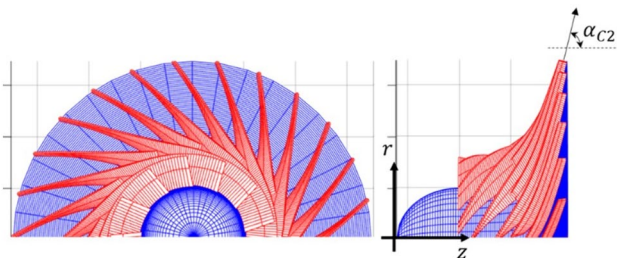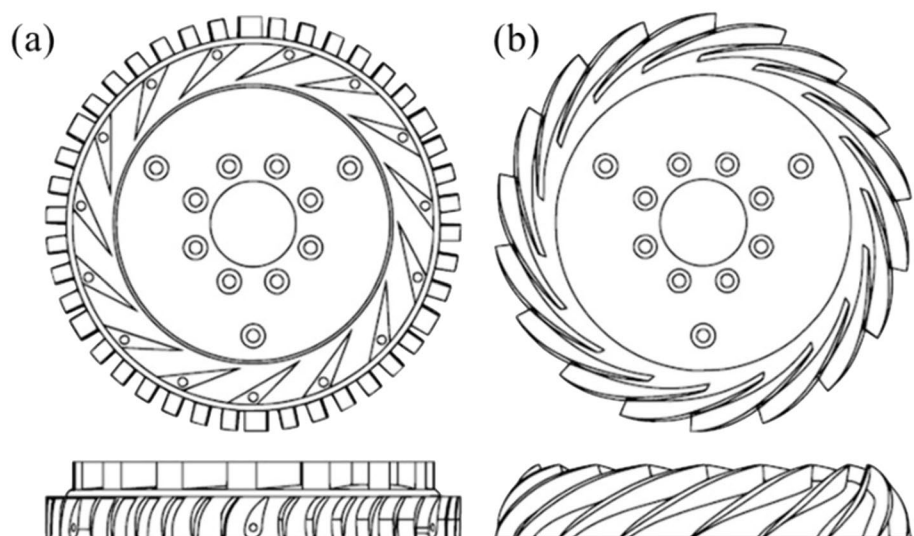

Fig. 1 Impeller meridional exit angle (α_{C2}) definition

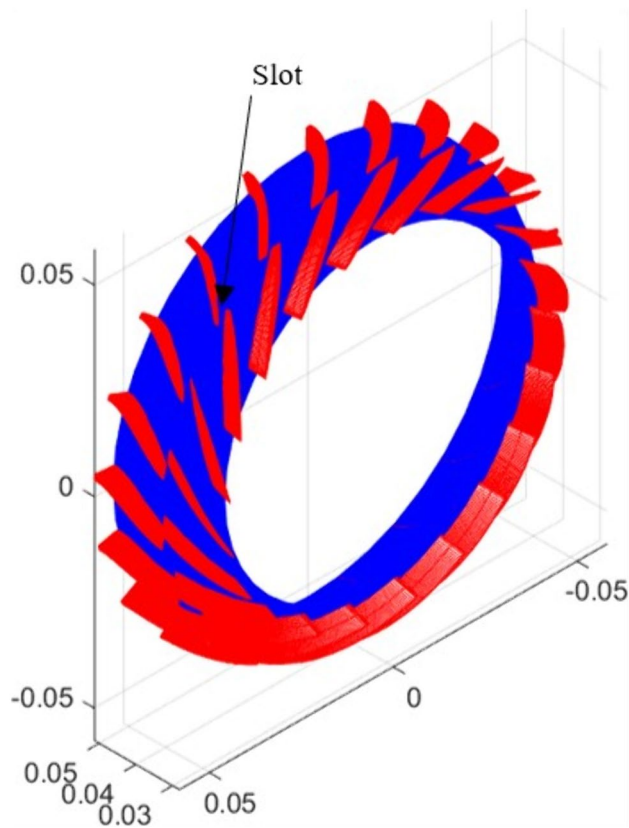Fig. 2 a Conventional diffuser configuration, b crossover diffuser configuration [12]

Fig. 3 Tandem Vane crossover diffuser schematic

length and a second vane relative tangential shift of 75% [15].

Van Eck et al. [16] evaluated methods to increase the choke margin of a mixed flow compressor fitted with a crossover diffuser. Various splitter vaned, tandem vaned and combinations of these were presented and these provided a marked increase in choke margin.

An upgrade of the CAT250-Gen1 compressor stage is proposed and numerically evaluated in this study. The upgraded compressor stage features a mixed flow configuration fitted with a crossover diffuser. To alleviate the reduced operating range attributed to the baseline single vane crossover diffuser, various diffuser modifications featuring tandem and splitter vane configurations are presented.

It is important to note that the current study forms part of a larger PhD study [15] evaluating the effect of various crossover diffuser configurations on the performance of the compressor stage of an MGT engine. The current paper is in fact the culmination of this study, where the findings of the larger study is tested on a real-world application, i.e. the CAT250TJ MGT engine. The details of the various diffuser configurations and their associated flow physics are described in detail in the PhD thesis document and are not repeated in this paper. The focus of the current paper is the

evaluation of the upgraded compressor of the CAT250TJ engine.

2 CFD Validation

In this study, performance validation is conducted using Numeca/FINE™ Turbo computational fluid dynamics (CFD) software. The 1D Application (App) [17] is used to design all the various compressor geometries evaluated in this study. The 1D App is an in-house developed MATLAB™-based mixed flow compressor design tool. The code is based on the one-dimensional mean line and loss model theory, primarily as proposed by Aungier [18]. The layout and working of the 1D App is detailed in Van Eck et al. [17]. As part of the design process, the 1D App exports a compressor geometry text file for CFD mesh creation in NUMECA AutoGrid5™. In AutoGrid5™, meshes are created in three grid levels of increasing coarseness, namely 000, 111, and 222. Flow simulation is typically commenced at a courser grid level, with the result used as an initial solution for the next finer grid level. This process increases the initial robustness of the flow solver. In this study, the medium grid level (111) is used, due to the much longer simulation time and larger memory requirement of the fine grid level (000) simulation. A grid independence check confirmed an insignificant difference between the 000 and 111 grid level.

The Spalart–Allmaras turbulence model is used, as recommended by Numeca™ for centrifugal compressors. The model is a one-equation model and provides economical computations in boundary layers, especially for external aerodynamic applications where adverse pressure gradients are encountered [19]. To ensure a proper boundary layer simulation when using the Spalart–Allmaras turbulence model, y^+ values are required to be below 10. For the CAT250TJ_BL, the 111 grid-level simulation achieved a maximum y^+ value of 9.8. This result further justifies the use and accuracy of the 111 grid level.
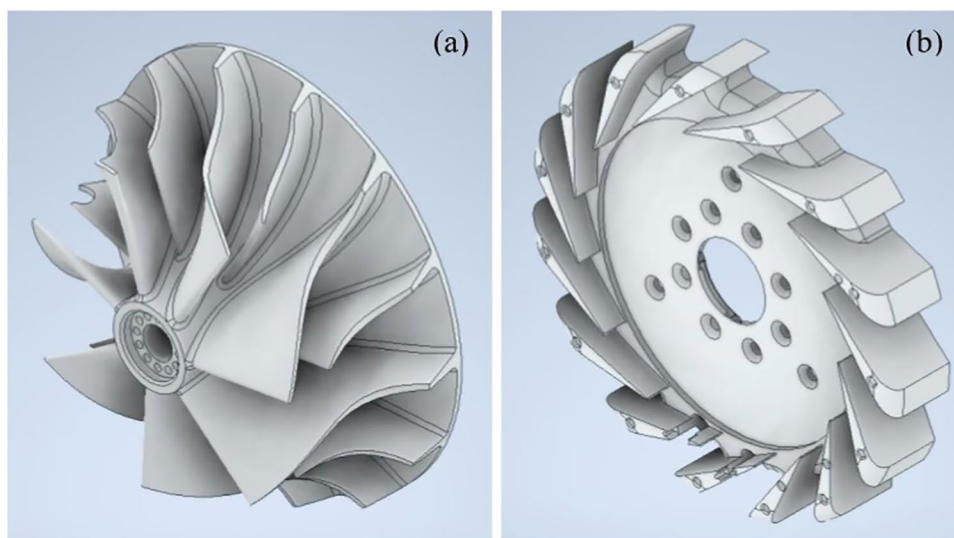
For this study, air as a calorically perfect gas is selected as the working fluid. The 'Flow Model' settings include a 'Steady' state Time Configuration and 'Turbulent Navier–Stokes' as a mathematical model. The 'Characteristic Length' and 'Characteristic Velocity' are based on the impeller exit geometry and tangential velocity. To ensure dynamic comparability, the inlet boundary conditions are kept constant at standard atmospheric conditions, namely 101,325 Pa and 288 K. The 'Velocity direction' selection is made, with the flow being purely axial approaching the inlet. The various operating curve points are determined by altering the mass flow rate (in kg/s) as an outlet boundary condition. The only exception here is the choke point, which is determined by setting the outlet boundary

condition to a static pressure well below the lowest achievable exit pressure to induce choke. The initial solution 'for turbomachinery' is used in most cases. 'Estimated static pressure' values are obtained from the 1D App performance calculations. The 'Maximum Number Of Iterations' are set to 6000, with the 'Convergence Criteria' specified as − 6. Convergence often transpires well before the maximum number of specified iterations are reached; in which case the solution terminates automatically. Convergence is achieved when either the global residual decreases below − 6 or the inlet and outlet mass flow rate converge to within at least 0.05%. In all cases, all other monitored variables should have stabilised. All other simulation flow settings are as presented by Van Eck et al. [17].

Fig. 4 CAT250TJ-Gen MGT Engine [20]

3 Baseline Test Compressor Design

The CAT250TJ-Generation1 (Gen1) (Fig. 4) is a 200 N MGT engine developed by Cape Aerospace Technologies in Cape Town [20]. Cape Aerospace Technologies is responsible for the design, testing and manufacture of various sized MGT engines. These are used in platforms such as model aircraft, high-speed target drones, UAVs, and even full-scale glider aircraft. These engines further feature a fuel atomising plasma ignition system, which enables fast and reliable engine start cycles, even at high altitudes. This system has been tested at altitudes up to 10,000 ft above mean sea level [21].

The CAT250TJ-Gen1 engine features a single-stage centrifugal compressor, annular combustor, and single-stage axial turbine. The compressor features a pure centrifugal impeller with 7 full and 7 splitter blades. The engine is designed for a full power operating point of 115,000 RPM at 0.45 kg/s mass flow rate. The compressor diffuser features 15 single vanes, having a wedge-type inlet shape and a straight outlet. A schematic of the impeller and diffuser is presented in Fig. 5.

The important CAT250TJ-Gen1 impeller and diffuser dimensions are provided in Tables 1 and 2 below.

The design process of the proposed compressor upgrade is commenced with a baseline compressor, featuring a mixed flow impeller and single vane crossover diffuser. Subsequent modifications incorporate the same impeller and diffuser meridional shape, but various diffuser vane modifications are employed. For the purpose of conciseness, the new baseline compressor upgrade is referred to as: CAT250TJ_BL.

The CAT250TJ_BL upgrade is designed using the 1D App. The CAT250TJ_BL is designed with the same interface dimensions of the CAT250TJ-Gen1 compressor

Fig. 5 CAT250TJ-Gen1 compressor schematic (**a**) impeller (**b**) diffuser

Table 1 CAT250TJ-Gen1 impeller dimensions

Symbol	Description	Unit	Value
r_{1h}	Inlet hub radius	mm	8.54
r_{1s}	Inlet shroud radius	mm	31.46
r_{2s}	Impeller outlet shroud radius	mm	41.5
b_2	Outlet width	mm	6.5
α_{C2}	Meridional exit angle	°	90
β_2	Blade exit angle (relative to axial direction)	°	17.56
z_{imp}	Impeller axial length	mm	31.48
Z_{imp}	Impeller number of blades	–	7
s_{CL}	Blade tip clearance	mm	0.568
$t_{B,max}$	Maximum blade thickness (shroud to hub)	mm	1–2
$t_{B,TE}$	Trailing Edge blade thickness (shroud to hub)	mm	1–2

Table 2 CAT250TJ-Gen1 diffuser dimensions

Symbol	Description	Unit	Value
r_{4h}	Outlet hub radius	mm	50
r_{4s}	Outlet shroud radius	mm	58.3
r_3/r_2	VG radius ratio	–	1.05
z_{diff}	Diffuser axial length	mm	19.8
Z_{diff}	Diffuser number of blades	–	15

Table 3 CAT250TJ_BL impeller dimensions

Symbol	Description	Unit	Value
$\dot{m}_{design}$	Design mass flow rate	kg/s	0.45
N_{design}	Design rotational velocity	RPM	115,000
r_{1h}	Inlet hub radius	mm	8.54
r_{1s}	Inlet shroud radius	mm	30.86
r_{2s}	Impeller outlet shroud radius	mm	42
b_2	Outlet width	mm	5.96
α_{C2}	Meridional exit angle	°	80
β_2	Blade exit angle (relative to axial direction)	°	30
z_{imp}	Impeller axial length	mm	33
Z_{imp}	Impeller number of blades (and splitters)	–	8
s_{CL}	Blade tip clearance	mm	0.3
TCR	Tip clearance ratio	–	0.0481
$t_{B,max}$	Maximum blade thickness (shroud to hub)	mm	1–1.5
$t_{B,TE}$	Trailing-edge blade thickness (shroud to hub)	mm	1–1.5
$L_{SB} : L_{FB}$	Splitter blade relative meridional length	–	0.815
θ_{R1}	Blade inlet rake angle	°	5
K	Blade rake parameter	°	0.387
$\dot{W}$	Required power	kW	79.72
BL	Blade loading at 0.45 kg/s (<0.9 required)	–	0.899

Table 4 CAT250TJ_BL diffuser dimensions

Symbol	Description	Unit	Value
r_{4h}	Outlet hub radius	mm	52.9
r_{4s}	Outlet shroud radius	mm	58.3
r_3/r_2	Vanless gap radius ratio	–	1.06
z_{comp}	Total axial length	mm	51.28
Z_{diff}	Diffuser number of vanes	–	23
$\Delta\alpha_{C2}$	Meridional kink angle	°	10
K_3	Diffuser vane shape factor	–	2.2
K_4	Diffuser vane shape factor	–	2.8
i_3	Vane inlet incidence angle	°	– 1
θ_{R3}	Vane inlet rake angle	°	10
β_4	Vane exit angle (relative to axial direction)	°	10
$t_{V,max}$	Maximum vane thickness	mm	1
$t_{V,TE}$	Trailing Edge vane thickness	mm	1
$2\theta_C$	Equivalent divergence angle (10°–11° required)	°	10.1
L	Blade loading (0.3–0.333 required)	–	0.3323
C_{U4}	Exit tangential velocity component	m/s	57

to ensure compatibility with the total engine. It features an 8-bladed (8 main and 8 splitter blades) impeller with a mixed flow angle (α_{C2}) of 80°. The baseline diffuser is a single-vane crossover diffuser with 23 vanes. The CAT250TJ_BL impeller and diffuser dimensions are provided in Tables 3 and 4 below. A 2D transformation plot of the CAT250TJ_BL diffuser and a 3D schematic of the whole compressor are provided in Fig. 6.

GasTurb™ gas turbine cycle software is used to model the design point on-engine performance of the baseline compressor configuration fitted to the CAT250TJ engine. Erario et al. [22] used GasTurb™ and GSP software to model the steady state and transient conditions of a micro gas turbine engine. The results were experimentally validated, and predicted performance errors were below 5%. The transient model was achieved even without access to exact compressor and turbine maps. Off-design points are normally achieved using map scaling. Erario et al. [22] were able to validate these transient and off-design points with experimental flight data and static test data.

For the current study, GasTurb™ software is chosen for two reasons. Firstly, it provides good engine modelling results for both design and off-design points and are widely regarded as one of the best software packages for this purpose [23]. Secondly, a GasTurb™ gas turbine cycle model of the CAT250TJ-Gen1 was developed by Schroder [24] and was therefore available for use in this study.

The on-engine performance evaluation of the CAT250TJ_BL configuration is conducted in two parts. Firstly, a simple compressor-turbine power matching evaluation is conducted. Secondly, a design point gas turbine cycle model of
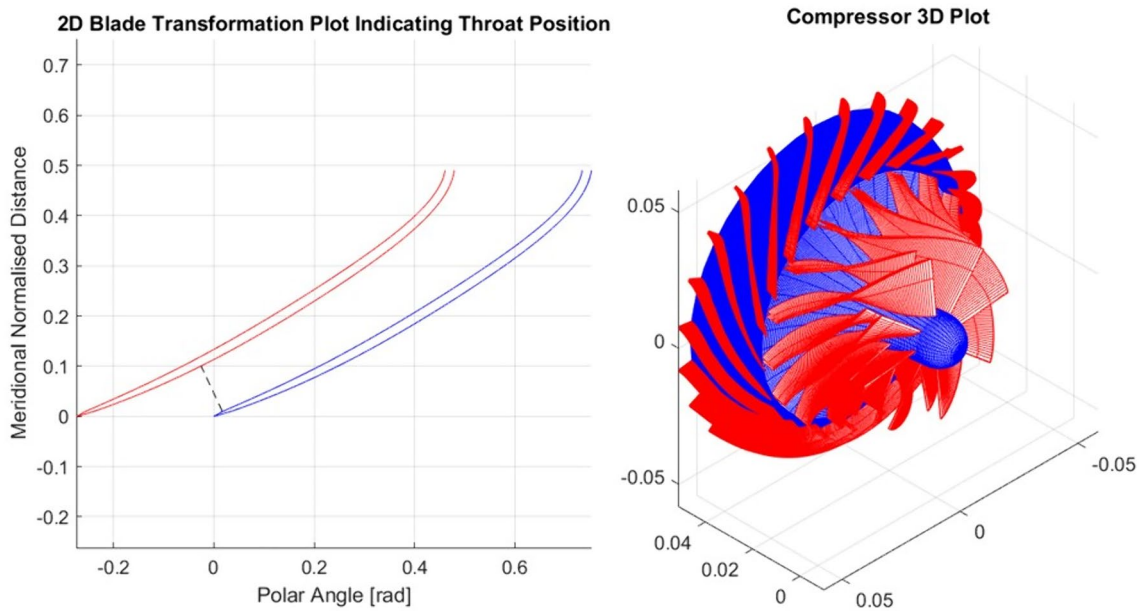
Fig. 6 CAT250TJ_BL diffuser 2D transformation plot and 3D compressor schematic
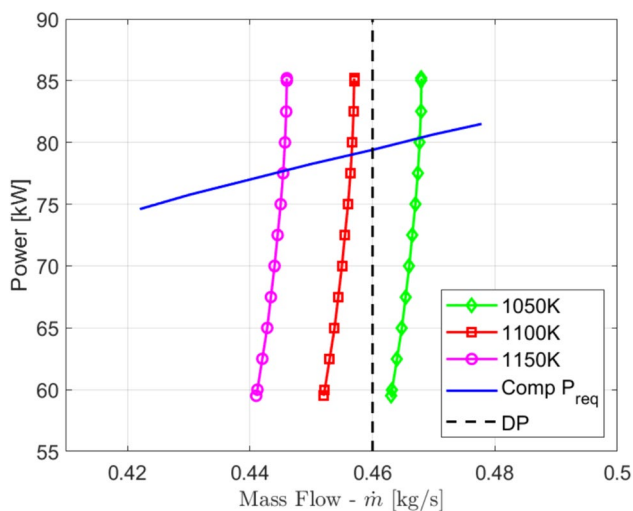

Fig. 7 CAT250TJ_BL compressor/turbine matching curves

the baseline configuration is conducted and compared to the available Gen1 model. These are explained separately below.

The CAT250TJ-Gen1 MGT engine was numerically modelled by Vass [25]. CFD performance and power matching curves for both the compressor and turbine was produced. The power required curve of the upgraded CAT250TJ_BL compressor is plotted over the turbine power available curves in Fig. 7. The turbine curves used in Fig. 7 was produced by Vass [25] using Numeca™ CFD software. The engine inlet conditions used were standard atmosphere parameters, which are the same as those used in the current study. Therefore, comparisons at real mass flow rates are feasible.

From Fig. 7 it is evident that the upgraded CAT250TJ_BL compressor design falls well within the turbine available power band at and around the design mass flow rate (DP). At the design point of $\dot{m} = 0.46$ kg/s (determined using the gas turbine cycle model—see next paragraph) the compressor input power requirement is approximately 79.5 kW at a turbine total inlet temperature of approximately 1080 K. It is interesting to note that the compressor of the CAT250TJ-Gen1 MGT engine exhibits a power requirement of 82.73 kW at $\dot{m} = 0.46$ kg/s. The upgraded baseline compressor therefore displays a lower power requirement.

The setup of the CAT250TJ-Gen1 in the gas turbine cycle model is described in detail in Schroder [24]. With standard atmospheric inlet conditions, the CAT250TJ-Gen1 gas turbine cycle model produces a nett static thrust of 213.2 N at maximum operating conditions. This compares well with the numeric and experimental results of 213.4 N and 214.9 N, respectively as determined by Vass [25]. For the CAT250_BL gas turbine cycle model, the input parameters are kept unchanged from the Schroder model, except for the compressor parameters. The updated compressor parameters at the converged design point of $\dot{m} = 0.46$ kg/s are summarised in Table 5.

The burner exit temperature of 1082 K compares well with the result of 1080 K obtained from the simple power matching evaluation. Important results at the operating point for the CAT250TJ_BL configuration are summarised in Table 6.

The CAT250TJ_BL configuration produces a 10.74% increase in static thrust compared to the Gen1 configuration. The lower power requirement of the baseline

Table 5 CAT2550TJ_BL GasTurb™ performance model compressor inputs

Input	Description	Unit	Value
ZW2Rstd	Inlet corrected mass flow	kg/s	0.46
ZP3q2	Compressor pressure ratio	–	3.711
T4_D	Burner exit temperature	K	1082
e23is	Compressor isentropic efficiency	–	0.762

Table 6 CAT250TJ_BL GasTurb™ operating point results

Parameter	Unit	Value
Static thrust	N	236.1
Compressor power requirement	kW	79.41
Specific fuel consumption	g/(kN s)	48.34

compressor also compares well with the simple power matching evaluation. It is further interesting to note that the baseline configuration provides a 9.66% better specific fuel consumption when compared to the Gen1 configuration.

The compressor design point performance used in the preceding gas turbine cycle model is extracted from the performance curves of the CAT250TJ_BL compressor. The performance curves of the CAT250TJ_BL compressor compared to the CAT250TJ-Gen1 compressor are provided in Fig. 8.

Before the results of Fig. 8 are analysed, it is important to firstly define an operating range. For the purpose of this paper, the operating range is quantified by means of stall margin (SM) and choke margin (*CM*):

$$SM = \frac{\dot{m}_o - \dot{m}_s}{\dot{m}_o}, \tag{1}$$

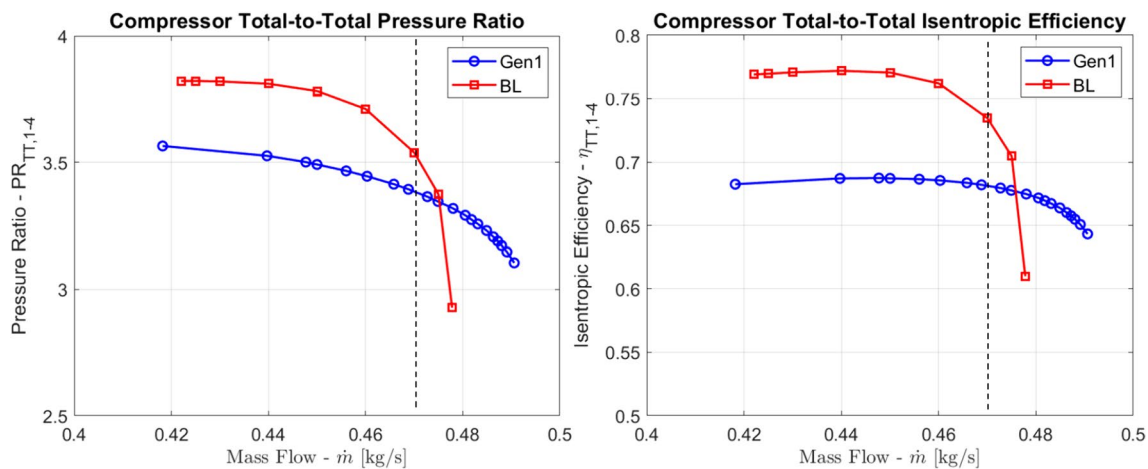$$CM = \frac{\dot{m}_c - \dot{m}_o}{\dot{m}_o}. \tag{2}$$

In Eqs. (1) and (2), $\dot{m}_o$ is the mass flow rate at the design (operating) point, $\dot{m}_s$ is the mass flow rate at the stall point and $\dot{m}_c$ is the mass flow rate at the choke point. During the compressor design phase, the determination of the stall/surge point is not a trivial matter. This is the case for both CFD and mean line modelling. For the purpose of this paper, a simple, conservative stall prediction method is employed. It is based on the stability criteria of Japikse and Baines [26]:

$$\frac{\partial PR}{\partial \dot{m}} = 0 \text{[Metastable conditions]}$$

$$\frac{\partial PR}{\partial \dot{m}} < 0 \text{[Stable conditions]}$$

$$\frac{\partial PR}{\partial \dot{m}} > 0 \text{[Unstable conditions]} \tag{3}$$

The gradient of the total-to-total pressure ratio performance curve is used to ascertain the stall/surge point. A positive gradient indicates the onset of unstable conditions and is used as the criteria for stall/surge point prediction. In essence, this is more of a 'instability' point, rather than a true 'stall/surge' point. For the purpose of this paper, this 'instability' point will be referred to as the 'stall' point. This instability criterion is used in both the CFD and mean line flow modelling phases.

Fig. 8 Comparative compressor performance curves—CAT250TJ-Gen1 and CAT250TJ_BL

From Fig. 8 it is immediately evident that the upgraded CAT250TJ_BL compressor provides a marked increase in design point performance. An increase of 8.3% and 12.1% is observed for design point total-to-total efficiency and pressure ratio, respectively. The upgraded baseline compressor does, however, display a reduced operating range. A relative reduction of 31.5% and 12.0% are observed for the choke margin and stall margin, respectively. In this performance comparison, the enhanced design point performance of a well-designed crossover diffuser compared to legacy type diffusers is highlighted. The crossover diffuser does, however, suffer from reduced operating range, as mentioned before. The current evaluation clearly validates these notions.

It is also pertinent to compare the diffuser exit tangential velocity (C_{U4}) of the baseline compressor with that of the Gen1 compressor. This is to ensure that the outlet tangential component is at least similar or smaller that the Gen1 compressor. Exit tangential velocity provides an indication of flow swirl exiting the impeller. A reduced swirl will lead to increased combustor efficiency. An outlet tangential velocity of 57 m/s is observed at the design mass flow rate for the CAT250TJ_BL compressor, which compares well with the value of 60 m/s of the Gen1 compressor.

The primary purpose of a diffuser is pressure recovery. The static pressure recovery coefficient (C_p) is a good parameter to gauge diffuser performance in terms of pressure recovery.

$$C_p = \frac{p_4 - p_2}{p_{02} - p_2}. \tag{4}$$

The static pressure recovery coefficient of the CAT250TJ_BL is determined to be 0.598, which is a substantial improvement over the 0.309 attributed to the CAT250TJ-Gen1 diffuser.

To expand the operating range of the upgraded CAT250TJ_BL compressor, selected operating range expansion methods discussed in Van Eck [15] are employed. These are discussed below.

4 Splitter Vane Configuration

The first baseline compressor diffuser modification that is evaluated is the simple splitter vane configuration. Van Eck [15] showed that the performance curves of a simple splitter vane diffuser configuration typically shift to the right, with an increased choke margin and decreased stall margin when compared to the baseline configuration. Van Eck [15] also recommends two methods to shift the 'wider' performance curves of the splitter vaned configuration to the left again. These include the design of the splitter vaned configuration

diffuser with a higher effective vane number, and/or design the modified compressor at a lower design mass flow rate. For the current evaluation, both these methods are employed.

The CAT250TJ_BL_S ('S' designating splitter vane) is designed with 15 splitter and 15 full vanes and a relative meridional splitter vane length of 0.8. This results in an effective vane number of 27. A lower design mass flow rate of 0.44 kg/s is also used. All other design parameters are kept unchanged from the baseline compressor. An initial evaluation of this configuration displayed an average vane loading (L) of 0.291, which is below the recommended value of 0.3 [18]. To alleviate this, the diffuser maximum vane thickness is increased from 1 to 1.2 mm. This results in the average diffuser vane loading increasing to the required 0.3.

The comparative performance curves of the baseline and splitter vaned configuration compressors are provided in Fig. 9 below.

A relative choke and stall margin increase of 37.8% and 7.15% is observed from the splitter vane configuration when compared to the baseline configuration. The methods employed to firstly enlarge the choke margin and subsequently move the performance curves to the left is clearly successful. A slight reduction in design point performance is observed. The total-to-total efficiency and pressure ratio display a reduction of 2.02% and 2.96%, respectively compared to the baseline configuration.

Compared to the CAT250TJ-Gen1 compressor, the CAT250TJ_BL_S still provides an increase of 6.32% and 5.10% in total-to-total efficiency and pressure ratio, respectively. This performance is displayed while still achieving a relative stall margin and choke margin within 5.66% and 5.64% of the Gen1 compressor. At 0.46 kg/s, the impeller power requirement of 81 kW still falls well inside the turbine power available curves.

An exit tangential velocity of 57 m/s is observed for the CAT250TJ_BL_S compressor. This is the same as for the baseline configuration. The CAT250TJ_BL_S also produces a diffuser static pressure recovery coefficient (C_p) of 0.545. This is slightly lower than the baseline diffuser, but still a marked improvement over the Gen1 diffuser.

The current evaluation shows that the CAT250TJ_BL_S configuration is a feasible option to be considered for upgrading the CAT250TJ-Gen1 MGT engine.

5 Low Solidity First Vane Row Configuration

The CAT250TJ_BL compressor is modified with a low-solidity front vane row. Two configurations are evaluated, namely a 25–75 and 22–75 configuration. All other parameters are kept unchanged from the baseline configuration. The comparative performance curves are provided in Fig. 10.
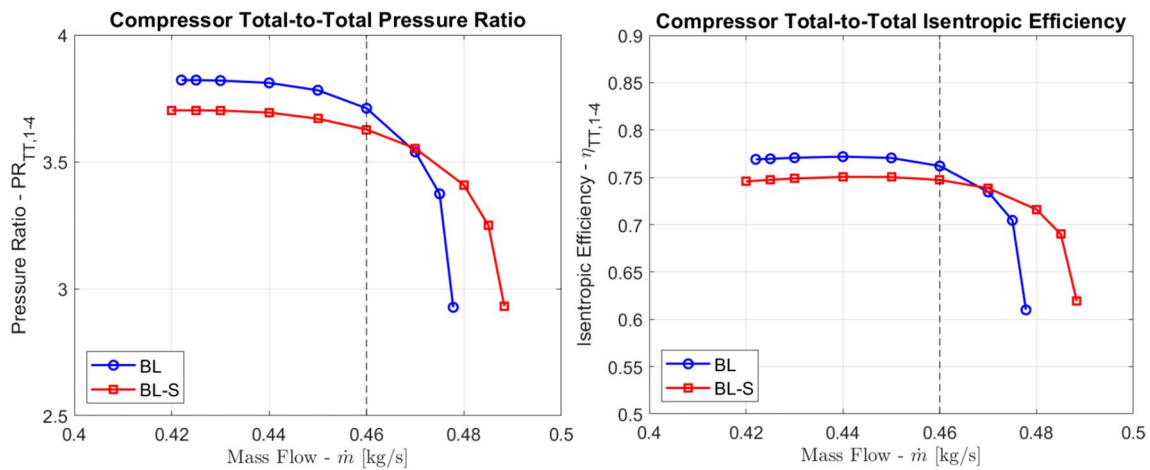
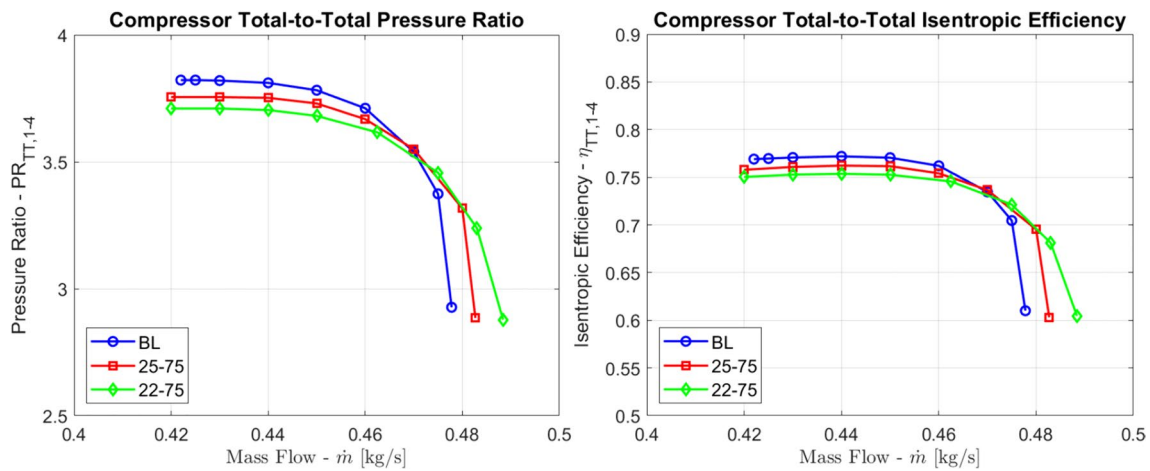**Fig. 9** Comparative compressor performance curves—CAT250TJ_BL and CAT250TJ_BL_S

Fig. 10 Comparative compressor performance curves—CAT250TJ_BL, CAT250TJ_BL_25-75 and CAT250TJ_BL_22-75

From Fig. 10 it is evident that both the 25–75 and 22–75 configurations display an increase in choke margin (17.6% and 38.1%, respectively) and stall margin (7.15% for both) compared to the baseline compressor. The 22–75 configuration displays slightly lower design point performance values compared to the 25–75 configuration. Design point performance for both is still within 1.79% and 2.67% for total-to-total efficiency and pressure ratio, respectively when compared or the baseline compressor.

Compared to the CAT250TJ-Gen1 compressor, the CAT250TJ_BL_22-75 provides an increase of 6.55% and 5.41% in total-to-total efficiency and pressure ratio, respectively. A relative stall margin and choke margin of 5.66% and 5.42% of the Gen1 compressor values are achieved.

An exit tangential velocity of 57 m/s is observed for the CAT250TJ_BL_22-75 and 25–75 compressors. This is the same as for the baseline configuration. The

CAT250TJ_BL_22-75 also produces a diffuser static pressure recovery coefficient (C_p) of 0.561, which is slightly lower than the baseline diffuser, but still substantially higher than for the Gen1 diffuser.

Based on the achieved results (particularly the increased choke margin) the CAT250TJ_BL_22-75 compressor is selected in favour of the 25–75 configuration. It provides a feasible option to be considered for upgrading the CAT250TJ-Gen1 MGT engine.

6 Reduced First Row Vane Number Configuration

The reduced first row vane number configuration is a unique layout that is presented in Van Eck [15]. It has the advantage of an increased choke margin due to a larger throat area

being created by the reduced front vane number. The slot, in combination with a shorter front vane also has a positive effect on stall margin.

As is the case with the simple splitter vane configuration, the reduced first-row vane number configuration has the effect that the performance curves expand and move to the right, compared to the baseline configuration. The two methods proposed to move the subsequent performance curves to the left (reduced design mass flow and increased effective vane number) are both implemented in the current evaluation. For this evaluation, a 40-75FRH (FRH designating first row half) configuration is selected, featuring a front row vane number of 17 and a rear row vane

number of 34. The resultant effective vane number is 27.2. The compressor is designed at 0.44 kg/s mass flow rate. A 2D transformation plot of the CAT250TJ_BL_40-75FRH diffuser and a 3D schematic of the whole compressor are provided in Fig. 11.

The comparative performance curves of the baseline and reduced first-row vane number configuration compressors are provided in Fig. 12 below.

The 40-75FRH configuration provides a 48.6% relative increase in choke margin and a 28.6% relative reduction in stall margin. A nett increase in operating range is therefore achieved. Compared to the baseline configuration, a design point performance reduction of 1.16% and 1.88% in
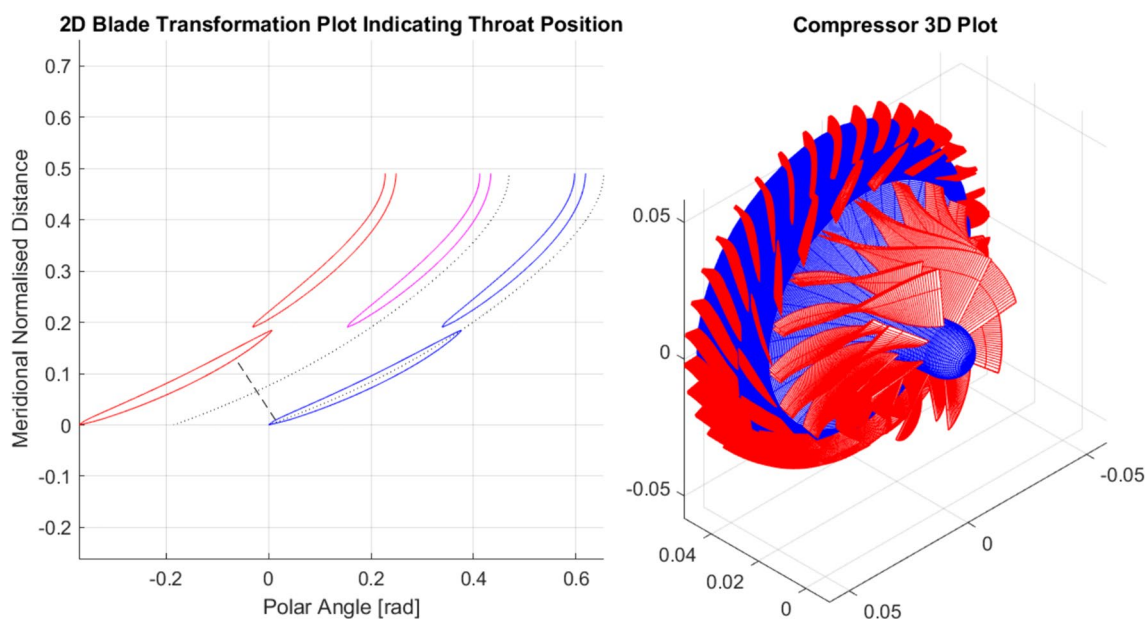

Fig. 11 CAT250TJ_BL_40-75FRH diffuser 2D transformation plot and 3D compressor schematic
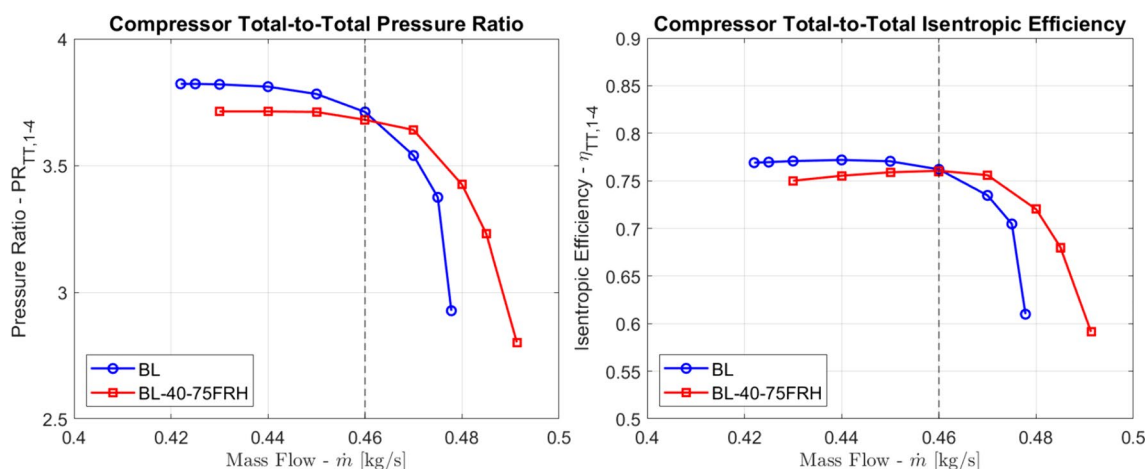

Fig. 12 Comparative compressor performance curves—CAT250TJ_BL and CAT250TJ_BL_40-75FRH

total-to-total efficiency and pressure ratio respectively is displayed, which is the best of all the modified configurations.

Compared to the CAT250TJ-Gen1 compressor, the CAT250TJ_BL_40-75FRH provides an increase of 7.18% and 6.27% in total-to-total efficiency and pressure ratio, respectively. Compared to the Gen1 compressor, the 40-75FRH configuration provides a relative increase in choke margin of 1.73%. A 37.1% reduction in stall margin is observed when compared to the Gen1 configuration.

An exit tangential velocity of 32 m/s is observed for the CAT250TJ_BL_40-75FRH compressor. This is a marked improvement compared to the baseline and Gen1 configurations. This tangential velocity decrease is attributed to the rearward movement of the slot. The resulting rearward movement of the separation point on the suction side of the rear vane consequently has a larger impact on the exit velocity distribution.

The CAT250TJ_BL_40-75FRH produces a diffuser static pressure recovery coefficient (C_p) of 0.596, which is similar to the baseline diffuser, and the best of all three modified diffusers. It provides a substantial improvement over the Gen1 diffuser.

At 0.46 kg/s, the impeller power requirement of 81.06 kW falls well inside the turbine power available curves. It is also notable that at an operating point of 0.46 kg/s, the 40-75FRH configuration displays similar performance than the baseline configuration.

The current evaluation shows that the CAT250TJ_BL_40-75FRH configuration is a feasible option to be considered for upgrading the CAT250TJ-Gen1 MGT engine.

7 Tandem/Splitter Combination Configuration

Like the reduced first vane row number configuration presented above, the tandem/splitter combination is a unique configuration presented by Van Eck [15]. It aims at combining the advantages of increased choke, attributed to the splitter configuration, and reduced exit tangential velocity, attributed to the rearward slot placement.

In a similar fashion as the reduced first vane row number configuration, the tandem/splitter combination configuration has the effect that the performance curves expand and shift to the right when compared to the baseline configuration. Again, both methods to alleviate this have been implemented in the current design. A S0.8_75-75 design (80% relative splitter vane length combined with 75–75 tandem configuration) is selected, featuring 30 rear vanes, 15 full front vanes and 15 splitter front vanes. This results in an effective vane number of 27. The impeller is inherited from the reduced front vane row configuration, which is designed at 0.44 kg/s design mass flow rate. A 2D transformation plot of the CAT250TJ_BL_S0.8_75-75 diffuser and a 3D schematic of the whole compressor are provided in Fig. 13.

The comparative performance curves of the baseline and tandem/splitter combination configuration compressors are provided in Fig. 14 below.

The S0.8_75-75 configuration provides a 63.3% relative increase in choke margin and a 10.2% relative reduction in stall margin. A nett increase in operating range margin of 26.2% is therefore achieved. A design point performance
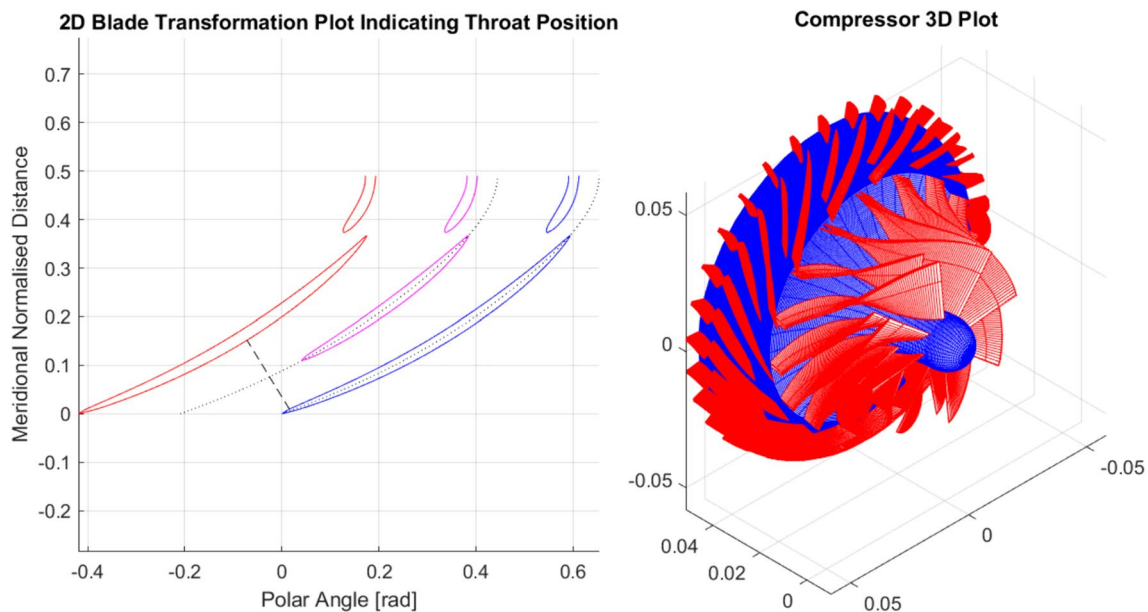

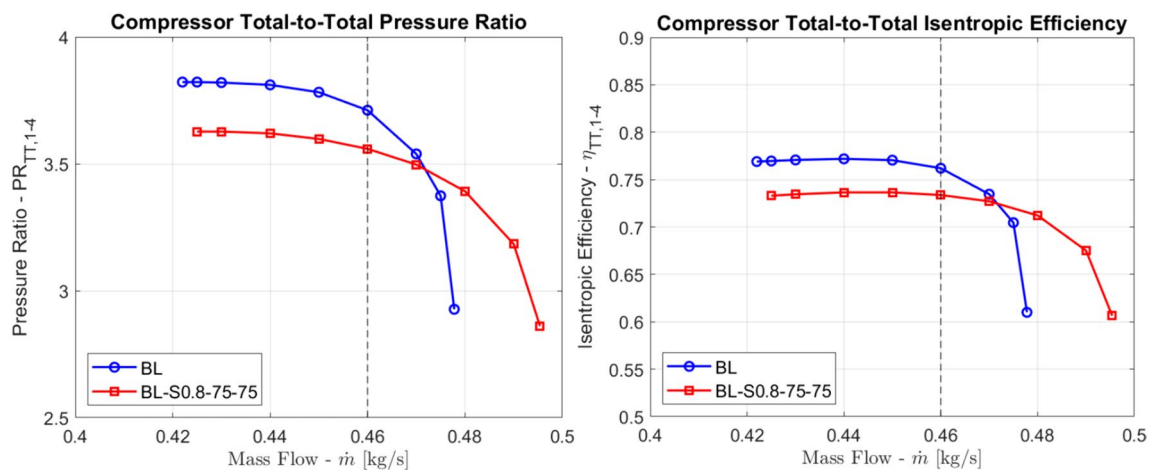**Fig. 13** CAT250TJ_BL_S0.8_75-75 diffuser 2D transformation plot and 3D compressor schematic

Fig. 14 Comparative compressor performance curves—CAT250TJ_BL and CAT250TJ_BL_S0.8_75-75

reduction of 3.40% and 4.86% in total-to-total efficiency and pressure ratio, respectively is displayed, which is the worst of all the modified configurations.

Compared to the CAT250TJ-Gen1 compressor, the CAT250TJ_BL_S0.8_75-75 provides an increase of 4.94% and 3.035% in total-to-total efficiency and pressure ratio, respectively. Compared to the Gen1 compressor, the S0.8_75-75 configuration provides a relative increase in choke margin of 11.9%, which is the best of all the modified configurations. A reduction of 21.4% in stall margin is observed when compared to the Gen1 configuration. At 0.46 kg/s, the impeller power requirement of 81.06 kW falls well inside the turbine power available curves.

An exit tangential velocity of 30 m/s is observed for the CAT250TJ_BL_S0.8_75-75 configuration. As is the case with the reduced front vane row configuration, the low exit tangential velocity is attributed to the rearward slot and its positive effect on delaying separation over the suction side of the rear vane.

The CAT250TJ_BL_S0.8_75-75 compressor produces a diffuser static pressure recovery coefficient (C_p) of 0.541, which is markedly superior to the Gen1 configuration. The current evaluation shows that the CAT250TJ_BL_S0.8_75-75 configuration is a feasible option to be considered for upgrading the CAT250TJ-Gen1 MGT engine.

8 Conclusion

The study focuses on a compressor upgrade for the CAT250TJ-Gen MGT engine. The upgrade process is initiated by the design of a baseline compressor featuring a standard, single-vane crossover diffuser. The superior performance of the crossover diffuser compared to legacy type diffusers is evident with the baseline design, which displays an increase of 8.3% and 12.1% for total-to-total efficiency and pressure ratio respectively, compared to the Gen1 configuration. As expected, the baseline configuration does, however, display a reduced operating range compared to the Gen1 configuration.

An on-engine evaluation is done by conducting a simple impeller-turbine power matching evaluation as well as a gas turbine cycle model design point comparison. The baseline configuration produces a 10.74% increase in static thrust and a 9.66% better specific fuel consumption when compared to the Gen1 configuration.

To expand the operating range of the baseline compressor, four modified diffuser configurations are presented. The combined performance curves of these are presented in Fig. 15. These are a simple splitter vaned configuration, a low solidity first row configuration, a reduced first-row vane number configuration, and a tandem/splitter combined configuration. All these configurations display an increased choke margin and operating range when compared to the baseline configuration. Apart from the 40-75FRH and S0.8_75-75 configurations, the modified configurations also display an increase in stall margin compared to the baseline configuration.

Compared to the baseline configuration, all but one (CAT250TJ_BL_S0.8_75-75) of the modified configurations display similar or slightly reduced (< 2% for efficiency and < 3% for pressure ratio) design point performance. These still equate to a design point performance increase of > 6.3% and > 5.1% for total-to-total efficiency and pressure ratio, respectively when compared to the Gen1 configuration. In terms of its primary purpose of pressure recovery, all the modified diffusers provide superior pressure recovery when compared to the Gen1 diffuser. All the modified diffusers display a pressure
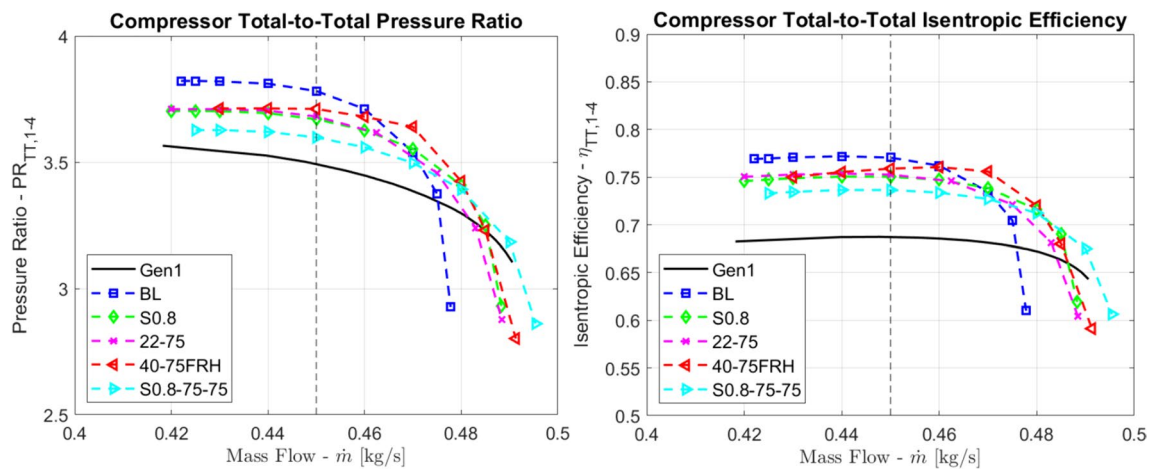
Fig. 15 Comparative performance curves—CAT250TJ

recovery coefficient in excess of 0.54, which is substantially higher than the 0.309 of the Gen1 diffuser.

The evaluation conducted in this study confirms the superior performance attributed to a crossover diffuser compared to legacy-type diffusers. The baseline compressor provides a marked increase in design point performance when compared to the Gen1 compressor. The current evaluation further confirms the feasibility of the proposed methods to expand the operating range of a crossover diffuser. All the modified configurations displayed wider operating ranges when compared to the baseline compressor, especially in terms of choke performance.

Declarations

References

1. Benini, E., Giacometti, S.: Design, manufacturing and operation of a small turbojet-engine for research purposes. Appl. Energy **84**(11), 1102–1116 (2007)
2. Phillips, M.S.: A computational investigation of the effects of inlet flow conditions on Vaned diffuser performance. Massachusets Institute of Technology (1997)
3. Dixon, S.L., Hall, C.A.: Fluid mechanics and thermodynamics of turbomachinery, 7th edn. Butterworth-Heinemann, Oxford (2014)
4. Goldstein, A.W.: Design and performance of experimental axial-discharge mixed-flow compressor impeller design theory, Cleveland, Ohio. [Online]. https://ntrs.nasa.gov/api/citations/19930085411/downloads/19930085411.pdf (1948). Accessed May 2020
5. Xu, X., Huang, X., Bi, D., Zhou, M.: An intellectual aerodynamic design method for compressors based on deep reinforcement learning. Aerospace **10**(171), 1–30 (2023). https://doi.org/10.3390/aerospace10020171
6. Çevik, M., Uzol, O.: Design optimization of a mixed-flow compressor impeller for a small turbojet engine. Aircr. Eng. Aerosp. Technol. **83**(3), 127–137 (2011)
7. Saravanamuttoo, H.I.H., Rogers, G.F.C., Cohen, H.: Gas Turbine Theory, 5th edn. Pearson, Harlow (2001)
8. Niculescu, M.L., Silivestru, V., Vizitiu, G., Danaila, S., Berbente, C.: Theoretical and numerical investigation of centrifugal and mixed compressor impellers. In: Proceedings of the 8th International Symposium on Experimental and Computational Aerothermodynamics of Internal Flows, pp. 1–7 (2007)
9. Zhang, Y.C., Kong, X.Z., Li, F., Sun, W., Chen, Q.G.: Performance improvement of a centrifugal compressor stage by using different vaned diffusers. IOP Conf. Ser. Mater. Sci. Eng. **52**(4), 1–6 (2013)
10. Musgrave, D.S., Plehn, N.J.: Mixed-flow compressor stage design and test results with a pressure ratio of 3:1. J. Turbomach. **109**(October), 513–519 (1987)
11. Kock, M.P.: Design of a cross-over diffuser for a mixed flow compressor impeller, Masters Thesis, Stellenbosch University, Stellenbosch. [Online]. https://scholar.sun.ac.za/items/3a0d13a5-d2d3-46ed-bf95-56b4bdd61b7c (2017). Accessed June 2018
12. Burger, C.: Design procedure of a compact aerodynamic crossover diffuser for micro gas turbine application. University of Stellenbosch (2016)

13. Zhao, Y., Li, J.: Study of the flow characteristics in multi-row vaned diffusers of a centrifugal compressor stage. Adv. Mech. Eng. **10**(9), 1–14 (2018)

14. Zhou, L., Wang, Z.X., Liu, Z.W.: Investigation on influence of design parameters for tandem cascades diffuser using doe method. Eng. Appl. Comput. Fluid Mech. **8**(2), 240–251 (2014)

15. Van Eck, H.: The effect of a crossover diffuser configuration on the performance of a mixed flow compressor stage for a micro gas turbine engine, Ph.D. Thesis, Stellenbosch University, Stellenbosch. [Online]. https://scholar.sun.ac.za/items/c41bed26-a69e-4cf1-9016-f771bfabfbe3 (2023). Accessed Jan 2024

16. Van Eck, H., Van der Spuy, S.J., Gannon, A.J.: Expanding the choke margin of a mixed flow compressor stage for a micro gas turbine engine. Int. J. Turbo Jet Engines (2023). https://doi.org/10.1515/tjj-2022-0060

17. Van Eck, H., Van der Spuy, S.J., Von Backström, T.W.: Development of a one-dimensional code for the initial design of a micro gas turbine mixed flow compressor stage. Int. J. Turbo Jet Engines **40**(s1), s207–s218 (2023). https://doi.org/10.1515/tjj-2022-0008

18. Aungier, R.H.: Centrifugal Compressors A Strategy for Aerodynamic Design and Analysis, 1st edn. Asme Press, New York (2000)

19. Versteeg, H.K., Malalasekera, W.: An Introduction to Computational Fluid Dynamics The Finite Volume Method, 2nd edn. Pearson Education, Harow (2007)

20. Cape Aerospace Technologies. https://www.capeaerospace.tech/ (2021). Accessed June 2021

21. Cape Aerospace Technologies: https://www.capeaerospace.tech/ (2022). Accessed June 2022

22. Erario, M.L., De Giorgi, M.G., Przysowa, R.: Model-based dynamic performance simulation of a microturbine using flight test data. Aerospace **9**(60), 1–18 (2022). https://doi.org/10.3390/aerospace9020060

23. Kurzke, J., Halliwell, I.: Propulsion and power an exploration of gas turbine performance modeling. [Online]. http://lib.ugent.be/catalog/ebk01:4100000004243679 (2018). Accessed June 2023

24. Schroder, B.: The development of a preliminary design process for the conversion of a micro gas-turbine engine to a turboshaft configuration, Masters Thesis, Stellenbosch University, Stellenbosch. [Online]. https://scholar.sun.ac.za/items/3b5376ee-2be8-4091-bb96-62e2d7feec0a (2023). Accessed Mar 2023

25. Vass, K.: Performance analysis of a micro gas turbine engine using computational fluid dynamics, Masters Thesis, Stellenbosch University, Stellenbosch. [Online]. https://scholar.sun.ac.za/items/54240093-8ba7-4be1-a2d3-0193ccfc3533 (2023). Accessed Mar 2023

26. Japikse, D., Baines, N.C.: Introduction to turbomachinery. Concepts ETI, Inc., Vermont (1997)